Growth of a predicted two-dimensional topological insulator based on InBi-Si(111)-sqrt[7]×sqrt[7]

Chia-Hsiu Hsu, Zhi-Quan Huang, Cho-Ying Lin, Gennevieve M. Macam, Yu-Zhang Huang, Deng-Sung Lin, Tai Chang Chiang, Hsin Lin, Feng-Chuan Chuang, and Li Huang

Phys. Rev. B **98**, 121404 — Published 6 September 2018

DOI: 10.1103/PhysRevB.98.121404

Growth of Predicted Novel Two-Dimensional Topological Insulator Based on InBi-Si(111)-$\sqrt{7}\times\sqrt{7}$

Chia-Hsiu Hsu,[1,*] Zhi-Quan Huang,[2,*] Cho-Ying Lin,[3,*] Gennevieve M. Macam,[2] Yu-Zhang Huang,[3] Deng-Sung Lin,[3,†] Tai Chang Chiang,[4,5] Hsin Lin,[6,7,8,‡] Feng-Chuan Chuang,[2,9,§] and Li Huang[1,¶]

[1]*Department of Physics, Southern University of Science and Technology, Shenzhen, Guangdong 518055, China*

[2]*Department of Physics, National Sun Yat-Sen University, Kaohsiung 804, Taiwan*

[3]*Department of Physics, National Tsing Hua University, No. 101, Section 2, Kuang-Fu Road, Hsinchu 30013, Taiwan*

[4]*Department of Physics, University of Illinois, Urbana, Illinois 61801-3080, United States*

[5]*Frederick Seitz Materials Research Laboratory, University of Illinois, Urbana, Illinois 61801-2902, United States*

[6]*Institute of Physics, Academia Sinica, Taipei 11529, Taiwan*

[7]*Centre for Advanced 2D Materials and Graphene Research Centre, National University of Singapore, Singapore 117546*

[8]*Department of Physics, National University of Singapore, Singapore 117542*

[9]*Multidisciplinary and Data Science Research Center, National Sun Yat-Sen University, Kaohsiung 804, Taiwan*

Abstract

Using combined scanning tunneling microscopy (STM) measurements and first-principles electronic structure calculations, we extensively studied the atomic and electronic properties of $\sqrt{7}$-InBi overlayer on Si(111). We propose and demonstrate an effective experimental process to successfully form a large well-ordered $\sqrt{7}$ surface by depositing Bi atoms on the In-Si(111)-4×1 substrate. The STM images exhibit a honeycomb pattern. After performing an exhaustive computational search, we identified the atomic structures of the surface at In and Bi coverages of 6/7 and 3/7 monolayers, respectively. We discovered a new trimer model with a lower energy than the previously proposed model. The simulated STM images of trimer models confirm the presence of the honeycomb pattern in accord with our experimental STM images. Most importantly, we found that the surface is robust, preserving the topologically non-trivial phase. Our edge state calculations verify that InBi overlayer on Si(111) is indeed a two-dimensional (2D) topological insulator (TI). Moreover, hybrid functional calculations result in band gaps up to 70 meV which is high enough for room temperature experiments. Our findings lay the foundation for the materials realization of 2D-TIs by growing InBi overlayer on Si(111) substrate.

INTRODUCTION

Since their recent discovery, two-dimensional (2D) topological insulators (TIs) have become a subject of intensive research. These novel materials, also known as quantum spin Hall (QSH) insulators, surprisingly possess spin-polarized, gapless edge states with Dirac-cone-like linear energy dispersion even though its interior is insulating [1–5]. Its versatile electronic properties makes it a feasible material to integrate into the modern silicon industry. Furthermore, they are also potential candidate materials for low energy consumption spintronics applications because its edge states are robust against nonmagnetic impurities. The existence of topological spin transport channels which was first demonstrated in the experiment is limited to quantum wells and measured at very low-temperatures, despite, the gaps could be up to 40 meV in theoretical prediction [6–8]. Thus, we are still challenged to search for new types of 2D TIs with band gaps large enough to support room-temperature applications.

QSH insulating phases have been discovered in numerous honeycomb materials [9–17]. Motivated by these discoveries and the experimental study of hydrogenated graphene [18], chemical functionalization such as hydrogenation and halogenation was utilized on honeycomb materials to explore for QSH phases [19–30]. Among them, numerous studies predicted potentially synthesized novel 2D TIs with band gaps large enough to exist at room temperature [12–16, 23–28]. However, experimental realizations generally require a substrate to synthesize 2D TIs and also ensure the predicted topological properties are achieved. Therefore, there is al so a need to further understand the effects of the substrate on free-standing TIs.

Huge amount of efforts and attempts have been made to realize the substrate-supported 2D-TIs [28–33]. A recent study predicted that planar honeycomb structures consisting of heavy metal elements, such as Bi with a large spin-orbit coupling (SOC), exist as TIs on SiC(0001) substrate [28]. This is because the bonding with the substrate leads to the removal of p_z bands in the Bi atom from the Fermi level and cause the system to induce a topological non-trivial phase. Later on, such hexagonal honeycomb Bi was successfully grown on SiC(0001) [31] and confirmed the theoretical prediction [28]. Another type of system composed of surface alloys formed through Bi or In atom adsorption to construct a planar honeycomb on Au/Si(111) was also predicted as a 2D TI [32, 33]. Unfortunately, the

synthesized system is not robust enough to maintain the non-trivial phase due to thermal buckling of the honeycomb [32, 33].

Among the previously cited research on honeycomb structures, we highlight the study on a new class of III-V honeycombs [15], such as InBi and GaBi, which exhibit topological insulating phases. These 2D materials can hold the topological phase after hydrogenation and with a Si(111) substrate [26]. These systems lack sufficient research attention as there is a very limited number of reports on successful experiments [34–36] Despite the difficulty, these type of surfaces are still deserving of in-depth exploration for its topological properties.

In this letter, we improve the growth of a stable and ordered surface alloy, InBi $\sqrt{7}\times\sqrt{7}$ (denoted as $\sqrt{7}$ throughout this paper) phase on Si(111) substrate [34] and explore the atomic, electronic, and topological properties of this system. Our experimental result showed that the $\sqrt{7}$ reconstruction is a stable state and was effectively achieved by depositing Bi on an In-Si(111)-4×1. Using the first-principles electronic structure calculations and scanning tunneling microscopy (STM), we systematically examined the atomic structures of $\sqrt{7}$ phase [34]. We found our newly identified trimer model to have a lower energy than the previously proposed one [34]. The STM measurement reveals the formation of a hexagonal pattern, which is consistent with our theoretical structural calculations. Most significantly, these two low energy lying trimer models (denoted as T1-T4 and T1-H3 models) are identified as topologically non-trivial materials. HSE06 [37] calculations reveal that the band gap is as large as 70 meV for a T1-T4 model. The orbital analysis of the electronic structure shows that the surface bands near the Fermi-level were composed of s-orbital In atoms and p_x and p_y orbitals of both In and Bi atoms. Finally, we theoretically demonstrated the edge state of semi-infinite InBi-Si(111)-$\sqrt{7}$ ribbon to validate its topological properties.

METHODS

The STM measurements were carried out in ultra-high vacuum (UHV) chamber with a base pressure below 2.0×10^{-10} Torr. The Si(111) substrate were cut from silicon wafer with a size of 2×10 mm^2. After 12 hours of outgassing at about 800 K, an atomically clean Si(111) surface was obtained by direct-current heating to ∼1450 K for a few seconds. The indium and bismuth atomic beams were generated by e-beam evaporators located about 7 cm away from the Si(111) substrate. The deposition rates are ∼0.17 ML/min, where 1.0

monolayer (ML) is 7.84×10^{14} atoms/cm^2 for Si(111).

The first-principles calculations were performed within the density functional theory framework [38] using generalized gradient approximation [39] and projector-augmented-wave potentials [40], as implemented in the *Vienna Ab-Initio Simulation Package* [41]. The kinetic energy cutoff was set at 400 eV. The system was simulated using a periodically repeating slab which consists of four Si bilayers, a reconstructed layer, and a vacuum space of ∼20 Å. The Si dangling bonds at the bottom of the slab were passivated using hydrogen atoms. The lattice constant of the lowermost Si bilayer was set to the theoretical value of 5.468 Å and the atoms situated here were not optimized. The remaining Si, In and Bi atoms were relaxed using conjugate gradient method until the residual force on each atom was smaller than 0.001 eV/Å. The surface Brillouin-zones (SBZ) of the $\sqrt{7}$ phases were sampled using Γ-centered 6×6×1 Monkhorst-Pack [42] grid. SOC was included for all the band structure calculations. The topology of the band structures were identified according to the method of Ref. [43] for calculating the Z_2 invariant in terms of the so-called n-field configuration of the system. The edge states were calculated from the Green function of semi-infinite model [44, 45] with the Hamiltonian derived from maximally-localized Wannier functions obtained via the WANNIER90 package [46].

RESULTS AND DISCUSSION

In our experiment, a two-step approach was employed to grow a full $\sqrt{7}$-InBi layer. First, a In-Si(111)-4 × 1 surface was prepared by depositing 1.0 ML In on Si(111)-7 × 7 at room temperature (RT), followed by annealing at 730 K for 60 s [47]. The second step was to deposit 0.4 ML Bi on the In-Si(111)-4 × 1 surface at RT, and subsequently anneal at 730 K for 60 s. This two-step approach can produce the $\sqrt{7}$-InBi phase that covers nearly the entire surface of the substrate as shown in Fig. 1(a). The theoretically proposed model for the $\sqrt{7}$-(In, Bi) structure contains ∼0.86 ML of In and ∼0.43 ML of Bi [34]. Our intensity analysis of synchrotron-radiation core-level photoemission (not shown here) for a similarly prepared surface shows that the In coverage is ∼0.8 ML and that of Bi is ∼0.4 ML. Apparently, indium atoms were partially desorbed during the annealing process.

In order to include an internal lattice reference from the substrate to build the $\sqrt{7}$ structure model, we have also grown a layer that consists both the $\sqrt{7}$-InBi and the 4 × 1-In

domains, as displayed in Fig. 1(b). The mixed-phase surface is obtained by co-deposition of 1.15 ML Bi and 0.86 ML In at RT and subsequent annealing at 770 K. The atomic arrangement of the $\sqrt{7}$ structure clearly exhibits a honeycomb structure, similar to that found in a previous report [34]. The corresponding Fourier transform image shown in Fig. 1(c) confirms the $\sqrt{7}$ periodicity. The lattice constant is $\sim 1.02 \pm 0.03$ nm which is in good agreement with the $\sqrt{7}$ periodicity (1.016 nm). In Fig. 1(d), an obvious hexagonal shape (outlined by blue circles and red lines) is observed. The angle between the $\sqrt{7}$ and $[1\bar{1}0]$ measures as 18.3°, close to the ideal value of 19.1°. In addition, the scanning tunneling spectroscopy (STS) measurements of $\sqrt{7}$-structure (Fig. 1(f)) is also consistent with the previous experimental study [34]

The $\sqrt{7}$ phase of InBi overlayer on Si(111) is composed of three Bi atoms and six In atoms. The previously proposed trimer model [34] defines a Bi trimer as a structure composed of three Bi atoms as shown in Fig. 2(b). The Bi trimers can be labelled based on its location, i.e. the positions of the three Bi atoms and the Bi trimer center. Hence, we identify the previously proposed trimer model as a T1-T4 model in Fig. 2(b). The labels T1 and T4 correspond to sites above the top and second layer of the first bilayer of the underlying Si(111) substrate, respectively. Moreover, we have also later considered the H3 site which is above the top position of the second bilayer of Si(111). To conduct an exhaustive structural search, we considered different possible combinations of the Bi atoms and Bi trimer center locations. Six structural models are generated by considering any two sites of T1, T4, and H3 sites. In addition, we also performed a random search by positioning three Bi atoms arbitrarily at any three positions from nine atomic sites on the alloy surface of the T1-T4 model and filled the rest by In atoms. In this way, we are able to generate 84 initial structures for relaxations. These two methods yielded a total of 90 initial structures for optimization using conjugate gradient method. After our systematic search, two kinds of low-energy structural models were found and summarized, namely the line model and trimer model. As expected, we found the structures from the previously proposed T1-T4 model [34], and also identified a new trimer model, T1-H3 (i.e. Bi atoms on T1 sites and Bi trimers on H3 sites) model, which has a lower energy of 21 meV. The top and side views of the newly found low-energy lying T1-H3 model are shown in Fig. 2(a). In contrast with the old T1-T4 model, the Bi atoms of the new T1-H3 model are likewise placed on T1 sites but the centers of the trimers are shifted from T4 to H3 sites. Other low-energy lying models are labelled

as the line models (labelled as LM-1 and LM-2) presented in Supplementary Figure S1 [48].

To determine the atomic structure, simulated STM images of the aforementioned four models are shown in Supplementary Figure S2 [48]. Only the simulated STM images of trimer models exhibit the honeycomb pattern. Simulated STM image of T1-H3 model with a sample bias of -1.0 eV shown in Fig. 1(e) has one brighter point in a unit cell. An obvious hexagonal shape (blue circles and red lines) consistent with the experimental results was observed. The adjacent indium trimers formed major and minor bright areas, indicated by large and small blue circles, respectively. For the rest of the discussion, we will focus on the trimer models.

After determining the atomic structures, we now proceed to the electronic properties of the $\sqrt{7}$ phase. The band structures of the two trimer models, T1-H3 and T1-T4 are shown in Figure 3 (a) and (b), respectively. The red lines denote the valence band maximun of the system. The band structures of these two trimer models are quite similar, We observe semi-metallic properties in both models but the band dispersions occur at different paths, since $\sqrt{7}$ has a threefold symmetry. Next, we analyzed the orbital contributions of the T1-H3 trimer model as presented in Fig. 3(c)–(e) because this model has a lower energy and is consistent with the STM images. We found that the main contribution of surface states near the Fermi level were from the p_x, p_y orbitals of Bi atom and s, p_x, p_y orbitals of In atoms as well as Si-p_z of the first Si bilayer. The valence band S_1 were composed of In-s and Si-p_z orbitals which indicate that an s-p_z bond was formed. Here, S_1 represents a pair of splitting bands with similar energy dispersion. The S_2 were contributed from the In-s and Bi-p_x and Bi-p_y. The conduction bands S_3 and S_4 were both composed of the p_x and p_y orbitals of In and Bi atoms but S_3 also includes In-s orbitals.

Since two trimer models (T1-H3 and T1-T4) and one line model (LM-2) are semi-metallic, we further calculated the Z_2 topological invariant. The result of Z_2 calculations are shown in Supplementary Figure S3 [48]. Interestingly, we found three models harboring topological non-trivial phases with Z_2=1, implying the robustness of topological phase.

Additional analysis using hybrid functional HSE06 calculations was used to correct the underestimated system band gap. Since HSE06 calculations require more computational resources, we would like to reduce the thickness of Si substrate as much as possible. Therefore, before further calculations, we are interested in the change of electronic structure when decreasing the number of bilayers on Si(111) substrate. Supplementary Figure S4 shows the

band structure of T1-H3 model with the substrate constructed from one to four Si BLs [48]. We found that the features of the system remains a semi-metal with the non-trivial topological phase ($Z_2 = 1$), but the gap and a few bands near the Fermi level show a slight change with the number of bilayers. For the purposes of reducing computational time and resource, two Si BLs were employed as the substrate for the HSE06 calculations. The band structures of two trimer models with different functionals, PBE and HSE06, are shown in Fig. 4(a) and (b) for T1-H3 and T1-T4, respectively. The band gap of T1-T4 model increased to 70 meV after HSE06 calculations. Due to the localization of the STS measurement, the experimental results are mainly dominated by the contribution of the Γ point in momentum (reciprocal) space. Therefore, we found that the gap at Γ point is 330(387) meV for T1-T4(T1-H3) model which is close to the experimental results of ∼500 meV.

We gain further insight into the non-trivial band topologies resulting from adsorbed In-Bi overlayer on Si(111)-$\sqrt{7}$ by carrying out edge state calculations. Here, we examine the T1-H4 model. A two-bilayer Si(111) substrate was used for the edge state calculation. Based on the results of HSE06 calculation, the Green's function of semi-infinite model was constructed to calculate the local density of states of the edge as shown in Figure 4 (c). The brighter(white) bands resulting from the edge connected the valence and conduction bands within the bulk gap. In particular, for each edge, an even number of edge states are seen to cross the Fermi level between two high symmetry points, Γ and π/a in Fig. 4(c), confirming that the system is indeed a 2D-TI.

CONCLUSIONS

In summary, we have grown and identified novel 2D Tls based on InBi overlayer on Si(111)-$\sqrt{7}$ by using STM measurements and first-principles electronic structure calculations. We demonstrated the formation of a well-ordered $\sqrt{7}$ reconstruction which can be attained by the deposition of Bi on In-Si(111)-4×1 substrate.We have systematically examined the atomic structures of $\sqrt{7}$ phase and found the new trimer T1-H3 model which has a lower energy of 21 meV than the previously proposed T1-T4 model. Our STM experiment confirmed the presence of a honeycomb pattern in InBi overlayer on Si(111)-$\sqrt{7}$ which matches our theoretical structure predictions. The topological non-trivial phase has been confirmed by calculating the Z_2 invariant and a set of edge states which connected the

valence and conduction bands. The HSE06 calculations reveal that the band gap is up to 70 meV for trimer models. Our findings show that InBi-Si(111)-$\sqrt{7}$ can provide a viable platform for hosting 2D topological phases, including the possibility of tuning the topological state via gating (out-of-plane electric field) [12] and/or further doping of the surface.

C. H. and L.H. acknowledges the support by the NSFC under Grant Nos. 11704176, 11404160, 11774142, and Shenzhen Peacock Plan Team under Grant No. KQTD2016022619565991. F.C.C. acknowledges support from the National Center for Theoretical Sciences and the Ministry of Science and Technology of Taiwan under Grant No. MOST-104-2112-M-110-002-MY3 and the support under NSYSU-NKMU joint research projects Nos. 105-P005 and 106-P005. He is also grateful to the National Center for High-performance Computing for computer time and facilities. D.S.L. acknowledges the financial support from the Ministry of Science and Technology of Taiwan under grant No. MOST-105-2112-M-007-018. H.L. acknowledges the Singapore National Research Foundation for support under NRF Award No. NRF-NRFF2013-03.

---

* These three authors contributed equally.

† dengsunglin@gmail.com

‡ nilnish@gmail.com

§ fchuang@mail.nsysu.edu.tw

¶ huangl@sustc.edu.cn

[1] A. Bansil, H. Lin, and T. Das, Rev. Mod. Phys. **88**, 021004 (2016).

[2] C. L. Kane and E. J. Mele, Phys. Rev. Lett. **95**, 146802 (2005).

[3] X. L. Qi, T. L. Hughes, and S. C. Zhang, Phys. Rev. B **78**, 195424 (2008).

[4] M. Z. Hasan and C. L. Kane, Rev. Mod. Phys. **82**, 3045 (2010).

[5] X.-L. Qi and S.-C. Zhang, Rev. Mod. Phys. **83**, 1057(54) (2011).

[6] B. A. Bernevig, T. L. Hughes, and S.-C. Zhang, Science **314**, 1757 (2006).

[7] M. König, S. Wiedmann, C. Brüne, A. Roth, H. Buhmann, L. W. Molenkamp, X.-L. Qi, and S.-C. Zhang, Science **318**, 766 (2007).

[8] A. Roth, C. Brüne, H. Buhmann, L. W. Molenkamp, J. Maciejko, X.-L. Qi, and S.-C. Zhang, Science **325**, 294 (2009).

[9] W.-F. Tsai, C.-Y. Huang, T.-R. Chang, H. Lin, H.-T. Jeng, and A. Bansil, Nat. Commun **4**, 1500 (2013).

[10] C.-C. Liu, W. Feng, and Y. Yao, Phys. Rev. Lett. **107**, 076802 (2011).

[11] Z.-Q. Huang, C.-H. Hsu, F.-C. Chuang, Y.-T. Liu, H. Lin, W.-S. Su, V. Ozoliņš and A. Bansil, New J. Phys. **116**, 115801 (2014).

[12] F.-C. Chuang, C.-H. Hsu, C.-Y. Chen, Z.-Q. Huang, V. Ozoliņš, H. Lin, and A. Bansil, Appl. Phys. Lett. **102**, 022424 (2013).

[13] Y. Xu, B. Yan, H.-J. Zhang, J. Wang, G. Xu, P. Tang, W. Duan, and S.-C. Zhang, Phys. Rev. Lett. **111**, 136804 (2013).

[14] M. Wada, S. Murakami, F. Freimuth, and G. Bihlmayer, Phys. Rev. B **83**, 121310 (2011).

[15] F.-C. Chuang, L.-Z. Yao, Z.-Q. Huang, Y.-T. Liu, C.-H. Hsu, T. Das, H. Lin, and A. Bansil, Nano Lett. **14**, 2505 (2014).

[16] Z.-Q. Huang, F.-C. Chuang, C.-H. Hsu, Y.-T. Liu, H.-R. Chang, H. Lin, and A. Bansil, Phys. Rev. B **88**, 165301 (2013).

[17] C. L. Kane and E. J. Mele, Phys. Rev. Lett. **95**, 226801 (2005).

[18] D. C. Elias, R. R. Nair, T. M. G. Mohiuddin, S. V. Morozov, P. Blake, M. P. Halsall, A. C. Ferrari, D. W. Boukhvalov, M. I. Katsnelson, A. K. Geim *et al.*, Science **323**, 610 (2009).

[19] J. O. Sofo, A. S. Chaudhari, and G. D. Barber, Phys. Rev. B **75**, 153401 (2007).

[20] J. C. Garcia, D. B. de Lima, L. V. C. Assali, and J. F. Justo, J. Phys. Chem. C **115**, 13242 (2011).

[21] C. H. Zhang, and S. S. Yan, J. Phys. Chem. C **116**, 4163 (2012).

[22] R. Wang, S. Wang, and X. Wu, J. Appl. Phys. **116**, 024303 (2014).

[23] B.-H. Chou, Z.-Q. Huang, C.-H. Hsu, F.-C. Chuang, Y.-T. Liu, H. Lin, and A. Bansil, New J. Phys. **16**, 115008 (2014).

[24] C.-C. Liu, S. Guan, Z. Song, S. A. Yang, J. Yang, and Y. Yao, Phys. Rev. B **90**, 085431 (2014).

[25] Z. Song, C.-C. Liu, J. Yang, J. Han, M. Ye, B. Fu, Y. Yang, Q. Niu, J. Lu, and Y. Yao, NPG Asia Materials **6**, e147 (2014).

[26] C. P. Crisostomo, L.-Z. Yao, Z.-Q. Huang, C.-H. Hsu, F.-C. Chuang, H. Lin, M. Albao, and A. Bansil, Nano Lett. **15**, 6568-6574 (2015).

[27] L.-Z. Yao, C. P. Crisostomo, C.-C. Yeh, S.-M. Lai, Z.-Q. Huang, C.-H. Hsu, F.-C. Chuang, H.

Lin and A. Bansil, Sci. Rep. **5**, 15463 (2015).

[28] C.-H. Hsu, Z.-Q. Huang, F.-C. Chuang, C.-C. Kuo, Y.-T. Liu, H. Lin, and A. Bansil, New J. Phys. **17**, 025005 (2015).

[29] M. Zhou, W.-M. Ming, Z. Liu, Z.-F. Wang, Y.-G. Yao, and F. Liu, Sci. Rep. **4**, 7102 (2014).

[30] M. Zhou, W. Ming, Z. Liu, Z.-F. Wang, P. Li, and F. Liu, Proc. Natl. Acad. Sci., **111**, 14378 (2014).

[31] F. Reis, G. Li, L. Dudy, M. Bauernfeind, S. Glass, W. Hanke, R. Thomale, J. Schäfer, and R. Claessen, Science, **357**, 287–290 (2017).

[32] B. Huang, K.-H. Jin, H. L. Zhuang, L. Zhang, and F. Liu, Phys. Rev. B **93**, 115117 (2016).

[33] F.-C. Chuang, C.-H. Hsu, H.-L. Chou, C. P. Crisostomo, Z.-Q. Huang, S.-Y. Wu, C.-C. Kuo, W.-C. V. Yeh, H. Lin, A. Bansil, Phys. Rev. B **93**, 035429 (2016).

[34] N. V. Denisov, A. A. Alekseev, O. A. Utas, S. G. Azatyan, A. V. Zotov, and A. A. Saranin, Sur. Sci. **651**, 105-111 (2016).

[35] D. V. Gruznev, L. V. Bondarenko, A. V. Matetskiy, A. N. Mihalyuk, A. Y. Tupchaya, O. A. Utas, S. V. Eremeev, C.-R. Hsing, J.-P. Chou, C.-M. Wei, A. V. Zotov, and A. A. Saranin, Sci. Rep. **6**, 19446 (2016).

[36] N. V. Denisov, A. A. Alekseev, O. A. Utas, S. G. Azatyan, A. V. Zotov, and A. A. Saranin, Surf. Sci. **666**, 6469 (2017).

[37] Krukau, A. V., Vydrov, O. A., Izmaylov, A. F. & Scuseria, G. E. Influence of the exchange screening parameter on the performance of screened hybrid functionals *J. Chem. Phys.* **125**, 224106 (2006).

[38] P. Hohenberg, and W. Kohn, Phys. Rev. **136**, B864 (1964). W. Kohn, and L. J. Sham, Phys. Rev. **140**, A1133 (1965).

[39] J. P. Perdew, K. Burke, and M. Ernzerhof, Phys. Rev. Lett. **77**, 3865 (1996).

[40] G. Kresse, and D. Joubert, Phys. Rev. B **59**, 1758 (1999).

[41] G. Kresse, and J. Hafner, Phys. Rev. B **47**, 558 (1993). G. Kresse, and J. Furthmüller, Phys. Rev. B **54**, 11169 (1996).

[42] H. J. Monkhorst, and J. D. Pack, Phys. Rev. B **13**, 5188 (1976).

[43] T. Fukui and Y. Hatsugai, J. Phys. Soc. Jpn. **76**, 053702 (2007).

[44] M. P. L. Sancho, J. M. L. Sancho and J. Rubio, J. Phys. F **15**, 851 (1985).

[45] Q.-S. Wu, S.-N. Zhang, H.-F. Song, M. Troyer, and A. A. Soluyanov, arXiv.1703.07789 (2017).

[46] A. A. Mostofi, J. R. Yates, Y.-S. Lee, I. Souza, D. Vanderbilt, and N. Marzari, Comput. Phys. Commun. **178**, 685–699 (2008).

[47] G. Lee, S.-Y. Yu, H. Kim, J.-Y. Koo, H.-T. Lee, and D. W. Moon, Phys. Rev. B **67**, (3), 035327 (2003).

[48] See Supplemental Material at http://XXX for the detail on atomic and band structure of line models, simulated STM images of discussed models, the band structures of different thickness of Si substrate, the calculation of Z_2 invariant.

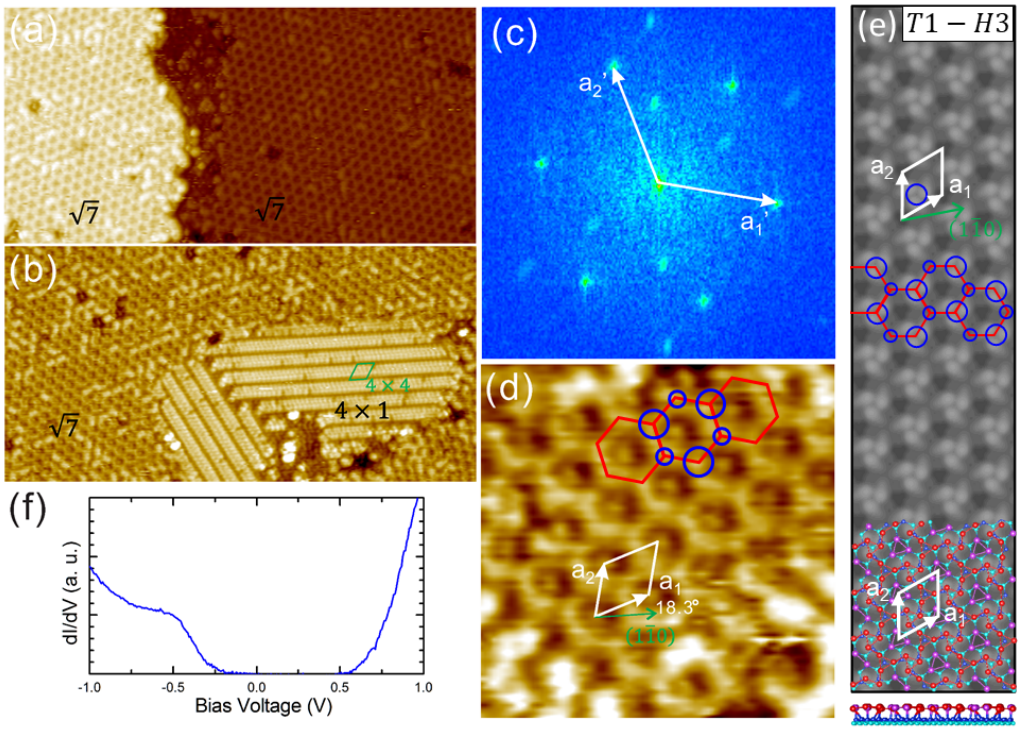

FIG. 1. Filled state STM images of the Si(111) surface after (a) the deposition of 0.4 ML Bi on the In-Si(111)-4×1 surface and (b) co-deposition of 1.2 ML Bi and 0.9 ML In at RT and subsequent annealing at 770 K. V_s = -1.1 V; I_t = 0.20 nA; size: 40×20 nm^2. The small thermal drift in the images is not corrected. In (b), the surface consists mainly of $\sqrt{7}$ domains and some 4×1 areas. (c) Fourier transform of (b). (d) 6×6 nm^2 zoomed-in STM image of the upper left area in (b). The white solid arrows in (c) point to first-order diffraction spots corresponding to the unit cell vectors in (d). (e) Simulated STM image of T1-H3 trimer model. The white line denotes a $\sqrt{7}$ unit cell in (d). (f) STS spectrum taken in a $\sqrt{7}$ area.

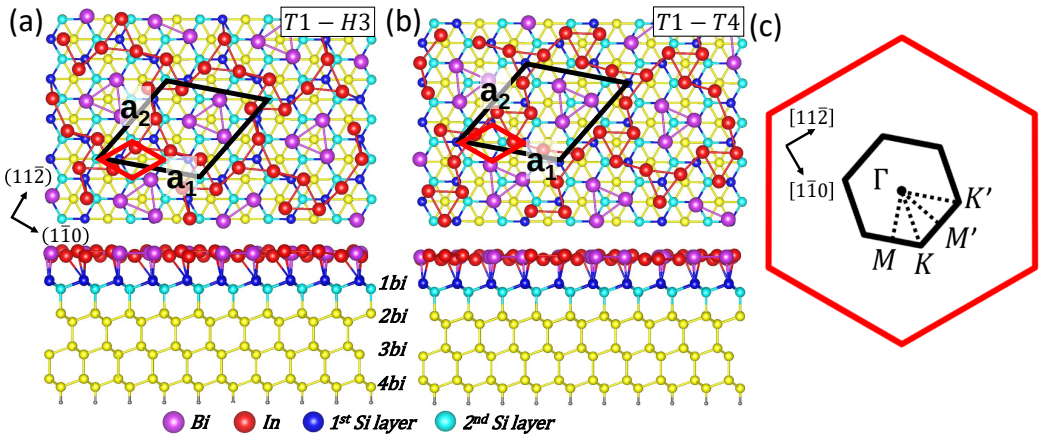

FIG. 2. Top and side views of structural models,(a) T1-H3 and (b) T1-T4, of InBi-Si(111)-$\sqrt{7}$. The black and red line marks the unit cell of the $\sqrt{7} \times \sqrt{7}$ and 1×1 phases, respectively. 2D Brillouin-zone (BZ) with specific symmetry points labeled is shown in (c). The BZ of $\sqrt{7} \times \sqrt{7}$ and 1×1 are indicated by black and red lines, respectively.

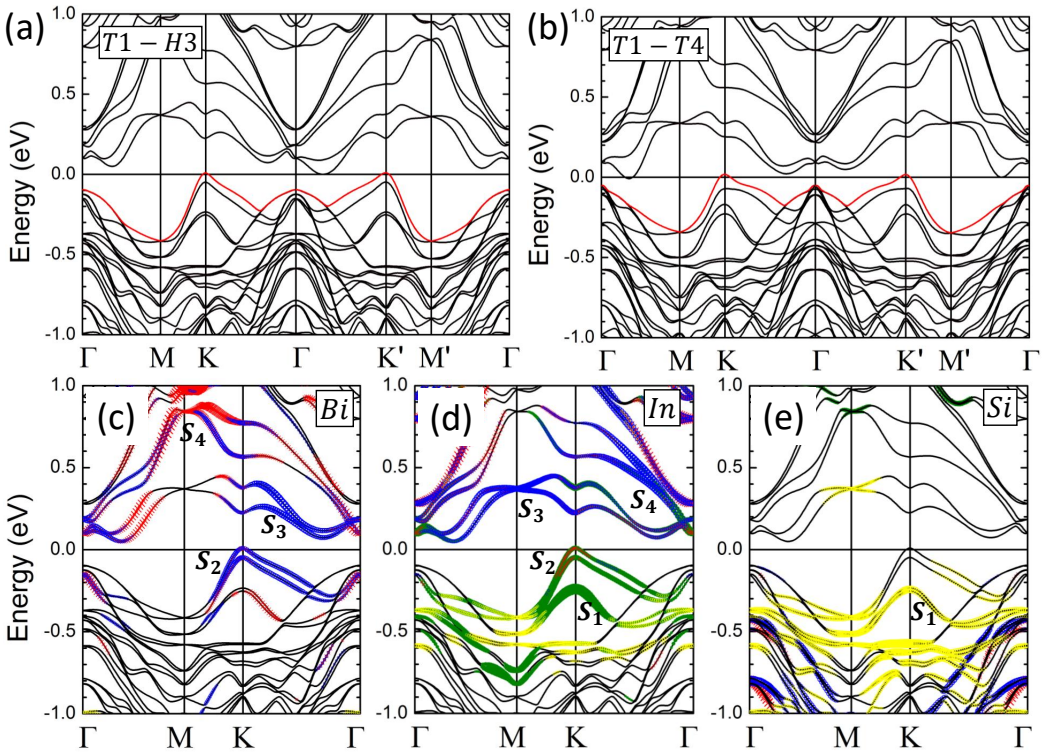

FIG. 3. Band structures of (a) T1-H3 and (b) T1-T4 trimer models. The valence band maximun is indicated by a red line. (c), (d) and (e) are the band structures of Bi, In, and first bilayer of the Si substrate, respectively, of the T1-H3 trimer model. The olive circles, red crosses, blue and yellow circles , respectively, denote the s-, p_x-, p_y- ,and p_z-orbital contributions.

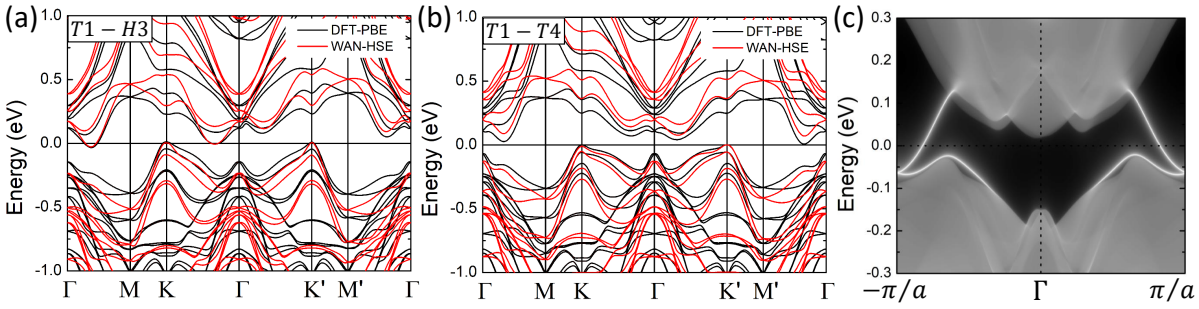

FIG. 4. (Color online) Band structures using PBE and hybrid functional (HSE06) including SOC calculations for (a) T1-H3 model and (b) T1-T4 model, respectively. Two Si BLs are used for the substrate. (c) is the edge band structure of T1-T4 model.